

# Microwave-Assisted One-Step Synthesis of FeCo/Graphene Nanocomposite for Microwave Absorption



Jianhui Peng, Zhiwei Peng, Liancheng Wang, Leixia Zheng, Zhongping Zhu, Guanghui Li and Tao Jiang

**Abstract** A high-performance microwave absorber composed of FeCo and graphene was prepared by a simple and rapid microwave-assisted one-step method. In the process, the metal precursors (iron hydroxide and cobalt hydroxide) and graphene oxide derived from graphite were transformed into FeCo and graphene, respectively, in only 12 min. Moreover, the FeCo nanoparticles were firmly dispersed on the surfaces of graphene nanosheets. The composition and structure of the FeCo/graphene nanocomposite were characterized by X-ray diffraction (XRD), Raman spectroscopy (RS), and transmission electron microscopy (TEM). It was found that with the filling ratio of only 10 wt% and the thickness of 2.2 mm, the nanocomposite showed the wide effective absorption bandwidth (less than  $-10$  dB) of 4.7 GHz with the minimum reflection loss of  $-12.56$  dB. The results of microwave absorption show that the nanocomposite is a potential candidate for high-performance microwave absorption.

**Keywords** Graphene · FeCo · Microwave-assisted synthesis  
Electromagnetic parameters · Microwave absorption

## Introduction

Electromagnetic wave is a double-edged sword which may bring both interests and damage to human beings. Therefore, any organizations and individuals using electromagnetic wave must ensure its rational application without leakage of electromagnetic power that will have influence on the health of humans and work of electronic devices [1, 2]. Developing microwave absorption material is an important and efficient method to solve electromagnetic pollution [3]. Generally, a material with good magnetic and dielectric properties has great wave absorption properties. For this reason, many efforts have been spent on developing appropriate composites

---

J. Peng · Z. Peng (✉) · L. Wang · L. Zheng · Z. Zhu · G. Li · T. Jiang  
School of Minerals Processing and Bioengineering,  
Central South University, Changsha 410083, Hunan, China  
e-mail: [zwpeng@csu.edu.cn](mailto:zwpeng@csu.edu.cn)

© The Minerals, Metals & Materials Society 2019  
B. Li et al. (eds.), *Characterization of Minerals, Metals, and Materials 2019*, The Minerals, Metals & Materials Series,  
[https://doi.org/10.1007/978-3-030-05749-7\\_33](https://doi.org/10.1007/978-3-030-05749-7_33)

of magnetic and dielectric materials [4, 5]. Graphene has lower resistivity, smaller density, high chemical stability and larger specific surface area than other common carbonaceous materials, and has received increasing attention in fundamental science and application [6–8]. With high permittivity and non-magnetic property, it has become an ideal choice as a substrate for metal nanoparticles to achieve a perfect match of magnetic performance and dielectric performance [9]. Metal nanoparticles (Ni [10], FeCo [11], FeNi [12], etc.) are a type of magnetic materials with high permeability, which are of beneficial to microwave absorption. Therefore, combining graphene with magnetic nanomaterials to form a nanocomposite will be an effective approach for further enhancement of microwave absorption [13, 14]. Guo et al. successfully prepared a  $\text{Co}_x\text{Ni}_y/\text{RGO}$  nanocomposite by a hydrothermal method. The  $\text{Co}_3\text{Ni}/\text{rGO}$  nanocomposite had the effective absorption bandwidth of ( $f_E$ ,  $\text{RL} < -10$  dB) of 5.61 GHz and the minimum reflection loss ( $\text{RL}_{\min}$ ) of  $-44.89$  dB at 12.22 GHz with a thickness of 2.5 mm and filling ratio of 40 wt% [15]. Liu et al. synthesized a Fe@Ni nanoparticles-modified graphene/epoxy composite by using a two-step method. The study showed that with the filling ratio of 10 wt% and the thickness of 2 mm, the  $\text{RL}_{\min}$  and  $f_E$  of the nanocomposite reached  $-22.7$  dB at 14.9 GHz and 5.5 GHz, (12.5–18 GHz), respectively [16]. These hybrid materials have shown enhanced microwave absorption. However, the complex synthetic processes for their fabrications will hinder their industrial applications.

In this study, microwave-assisted one-step synthesis of the FeCo/graphene nanocomposite was explored. The resultant nanocomposite showed good microwave absorption due to its favorable nanostructure and morphology.

## Experimental

### *Materials*

All chemical reagents used in this experiment including natural graphite powder ( $<48$   $\mu\text{m}$ ), sulphuric acid ( $\text{H}_2\text{SO}_4$ ), potassium permanganate ( $\text{KMnO}_4$ ), sodium nitrate ( $\text{NaNO}_3$ ), hydrogen peroxide ( $\text{H}_2\text{O}_2$ ), ethylene glycol (EG), cobaltous chloride ( $\text{CoCl}_2$ ), ferric chloride ( $\text{FeCl}_3$ ), sodium hydroxide ( $\text{NaOH}$ ), and ethanol were of analytical grade and used as received without further purification.

### *Preparation of the FeCo/Graphene Nanocomposite*

For preparation of the FeCo/graphene nanocomposite, 100 mg of graphene oxide (GO), which was preliminarily prepared by the Hummers method using the natural graphite powder as starting material [17], was added into 80 mL of EG under ultrasonication for 1 h. Meanwhile, 182.5 mg of  $\text{FeCl}_3$  and 146.1 mg of  $\text{CoCl}_2$  were

added into 20 mL of EG with ultrasonication for 0.5 h. Subsequently, the solution containing the metal ions was added to the above GO solution drop by drop under ultrasonication for 0.5 h to form a mixed solution. The mixture was stirred for 4 h at room temperature. The pH value of the suspension was adjusted to 13 by adding 7.5 mol/L NaOH. The mixture was stirred for 1 h at room temperature. Then, the reaction mixture was heated at 190 °C for 12 min using a microwave reactor (MAS-II, Sineo Microwave Chemistry Technology Co. Ltd., Shanghai, China) at the power level of 500 W. The resulting precipitate was filtered, washed with deionized water and ethanol, and finally dried in a vacuum oven at 60 °C for 12 h.

### Characterization

The phase compositions of the synthesized materials, including the FeCo/graphene nanocomposite, were identified by X-ray diffraction (XRD) using a PANalytical Empyrean powder X-ray diffractometer with Cu K $\alpha$  radiation ( $\lambda = 0.154178$  nm) in the scattering range ( $2\theta$ ) of 5–80°. The molecular structures of the materials were determined by Raman spectroscopy (RM) using a confocal Raman microscope (Renishaw RM 2000) equipped with a He–Ne laser ( $\lambda = 532$  nm). The microstructures of the materials were characterized by transmission electron microscopy (TEM) on a Cu grid using a Tecnai G<sup>2</sup> F20 microscope at an accelerating voltage of 100 kV. The electromagnetic parameters (complex relative permittivity and permeability) of the synthesized materials were measured by the coaxial line method using an Agilent N5230A vector network analyzer in the frequency of 2–18 GHz. Before the measurement, the as-prepared sample powders were homogeneously mixed with paraffin (the mass fraction of the FeCo/graphene nanocomposite was 10 wt%), and then the mixture was pressed into circular ring with 3.0 mm inner diameter, 7.0 mm outer diameter and 2.0 mm thickness. Then, the sample ring was embedded into a copper holder which was then connected to the waveguide of the equipment for measuring the electromagnetic parameters. To determine the microwave absorption properties of each synthesized material, the corresponding reflection loss (RL) was calculated by the following equations [18]:

$$RL \text{ (dB)} = 20 \times \log \left| \frac{Z_{in} - Z_0}{Z_{in} + Z_0} \right| \quad (1)$$

$$Z_{in} = Z_0 \times \sqrt{\frac{\mu_r}{\epsilon_r}} \times \tanh \left[ j \times \frac{2 \times \pi \times f \times d}{c} \times \sqrt{\mu_r \times \epsilon_r} \right] \quad (2)$$

$$Z_0 = \sqrt{\frac{\mu_0}{\epsilon_0}} \quad (3)$$

where  $Z_{in}$  is the input impedance of the material;  $Z_0$  is the input impedance of the free space;  $\epsilon_r$  ( $\epsilon_r = \epsilon_r' - j\epsilon_r''$ ) is the complex relative permittivity of the material;  $\mu_r$  ( $\mu_r = \mu_r' - j\mu_r''$ ) is the complex relative permeability of the material;  $c$  is the velocity

of electromagnetic waves in free space;  $f$  is the frequency and  $d$  is the thickness of the material.

## Results and Discussion

The phase compositions of the GO and FeCo/graphene nanocomposite are shown in Fig. 1a. For GO, the sharp diffraction peak at  $10.7^\circ$  corresponded to its (001) crystal plane, indicating the presence of oxygen groups on the GO surface [19]. For the FeCo/graphene nanocomposite, the two diffraction peaks at  $2\theta = 44.8^\circ$  and  $65.2^\circ$  corresponded to the (110) and (200) planes of cubic FeCo (JCPDS card no. 44-1433). Meanwhile, a peak at  $24.5^\circ$  for graphene was observed, and there was no obvious diffraction peak of GO. It could be deduced that GO was reduced to graphene and FeCo was successfully synthesized.

For further determination of the change of carbon structure during the synthesis, the molecular structures of the GO and FeCo/graphene nanocomposite were determined by Raman spectroscopy, as shown in Fig. 1b. Generally, the G peak usually represents the in-plane vibration of  $sp^2$  carbon atoms, and D peak represents the disorder in the graphitic structure. In addition, the intensity ratio of the D peak to G peak ( $I_D/I_G$ ) has been widely applied to identify the molecular structures of the carbon-based materials [20]. The values of  $I_D/I_G$  of the GO and FeCo/graphene nanocomposite were 0.92 and 0.81, respectively. The results indicated a higher quantity of ordered graphite crystal structure in the FeCo/graphene nanocomposite compared with GO. Furthermore, the increased C–C  $sp^2$  bond of the nanocomposite was expected to improve the conductivity and thus the conductive loss of the material [21].

The structure and morphology of the FeCo/graphene nanocomposite were characterized by transmission electron microscopy (TEM), as shown in Fig. 2. In Fig. 2a, the graphene appeared to be transparent as thin films with enormous surface area and a wrinkled morphology. The crystallite size of the spherical FeCo nanoparticles was

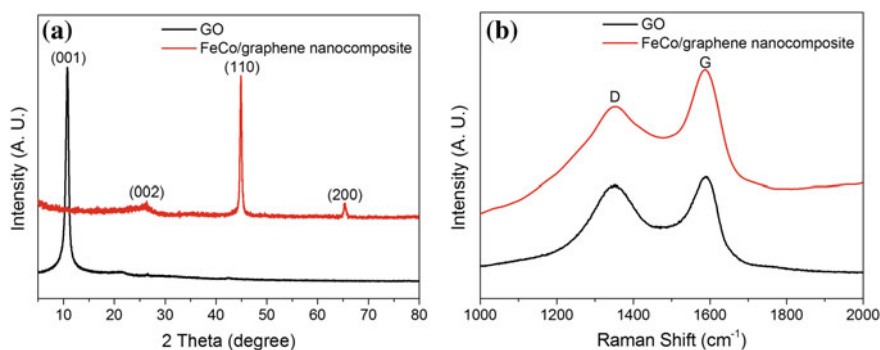


**Fig. 1** a XRD patterns and b Raman spectra of the GO and FeCo/graphene nanocomposite

40.27 nm on average, indicating its uniform morphology and crystallite size. Surprisingly, these nanoparticles were firmly anchored on the surface of graphene, and the nanoparticles were separated from each other without any aggregation. The morphology consisted of the large specific surface area of graphene and uniform dispersion of FeCo nanoparticles would promote multiple wave reflection in the nanocomposite. In Fig. 2b, the lattice distance of the FeCo nanoparticles in the FeCo/graphene nanocomposite was measured to be 0.200 nm and was indexed to the (110) crystallographic plane of FeCo. The selected area electron diffraction (SAED) pattern of the FeCo/graphene nanocomposite (Fig. 2c) showed the lattice fringe spacing of 0.200 nm corresponded to the (110) plane of the body-centered cubic (bcc) structure of FeCo. The mass percentage and atomic percentage of the FeCo/graphene were measured by the energy dispersion spectrum (EDS), as shown in Fig. 2d. The atomic ratio of the C, O, Fe, and Co was found to be 252:6:5:5. These results further confirmed the successful synthesis of the FeCo/graphene nanocomposite.

The microwave absorption properties of the FeCo/graphene nanocomposite can be determined by the measurements of complex relative permittivity ( $\epsilon_r = \epsilon_r' - j\epsilon_r''$ ) and the complex relative permeability ( $\mu_r = \mu_r' - j\mu_r''$ ) in the frequency range of 2.0–18.0 GHz. Figure 3a shows the frequency dependences of the real part ( $\epsilon_r'$ ) and imaginary part ( $\epsilon_r''$ ) of the complex relative permittivity of the FeCo/graphene nanocomposite. The  $\epsilon_r'$  value decreased gradually from 5.76 to 4.63 and the  $\epsilon_r''$  value increased from 0.45 to 1.31, respectively, in the frequency range of 2–18 GHz. Figure 3b shows the frequency dependences of the real part ( $\mu_r'$ ) and imaginary part ( $\mu_r''$ ) of the complex relative permeability of the FeCo/graphene nanocomposite. The  $\mu_r'$  value of the FeCo/graphene nanocomposite was about 1.77 at 2 GHz and then declined rapidly to 0.99 at 18 GHz. In addition, the  $\mu_r''$  values formed a broad resonance peak in 2–6 GHz which was believed to cause magnetic loss.

To demonstrate the microwave absorption properties of the FeCo/graphene nanocomposite, a three-dimensional map and a two-dimensional (contour) map of RL of the FeCo/graphene nanocomposite with different thicknesses are shown in Fig. 4. It can be clearly seen that the RL values of two RL peaks were  $-14.23$  dB at a thickness of 2.0 mm and  $-13.88$  dB at a thickness of 2.5 mm, respectively. This phenomenon indicated that when the thickness varied in the range of 1.9–2.8 mm, the nanocomposite had better absorption properties in the frequency ranges of 11.9–14.1 GHz and 16.5–17.7 GHz, respectively. According to Fig. 4b, the  $f_E$  reached 4.7 GHz (from 13.0 to 17.7 GHz) with a thickness of 2.2 mm. Considering the large absorption bandwidth, strong absorption and small thickness for practical applications, 2.2 mm was considered to be optimal for the FeCo/graphene nanocomposite. With this thickness, the nanocomposite exhibited a  $RL_{\min}$  of  $-12.56$  dB and a wide  $f_E$  of 4.7 GHz.

In order to understand the possible mechanism giving rise to the enhanced microwave absorption properties of the FeCo/graphene nanocomposite, the dielectric loss tangent ( $\tan\delta_\epsilon = \epsilon_r''/\epsilon_r'$ ) and the magnetic loss tangent ( $\tan\delta_\mu = \mu_r''/\mu_r'$ ) were calculated. The results are shown in Fig. 5. In Fig. 5a, the values of  $\tan\delta_\mu$  were larger than those of  $\tan\delta_\epsilon$  from 2.0 to 5.7 GHz. Hence, the magnetic loss greatly contributed to the microwave attenuation of the FeCo/graphene nanocomposite in 2.0–5.7 GHz. As is well known, the magnetic loss of magnetic solids is mainly originated from

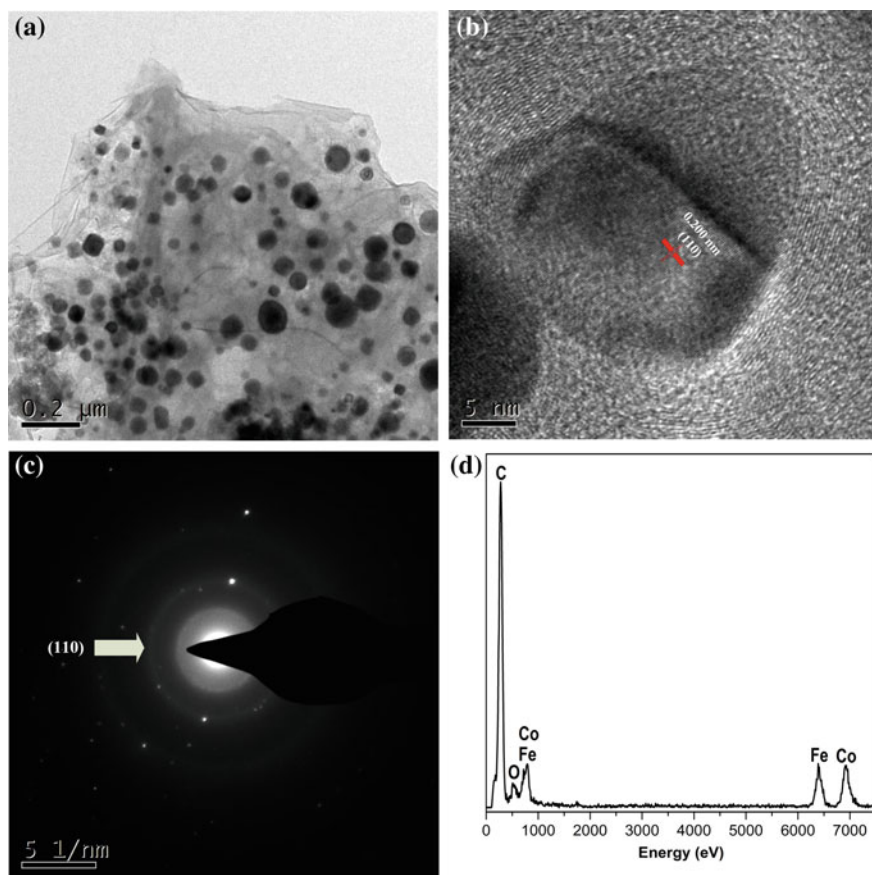


**Fig. 2** **a** TEM image, **b** HRTEM image, **c** SAED pattern and **d** EDS spectrum of the FeCo/graphene nanocomposite

the natural ferromagnetic resonance, domain wall resonance, eddy current effect and hysteresis loss [22]. The hysteresis loss is attributed to irreversible magnetization and is negligible in a weak applied field. The domain wall resonance contribution is also ignorable because it usually happens at 1–100 MHz, far below the present measured frequency range [22]. The eddy current effect is usually expressed as  $\mu_r'' \approx 2\pi\mu_0(\mu_r')^2\sigma d^2 f/3$ , ( $\mu_0$  is the vacuum permeability,  $d$  is the diameter of particles, and  $\sigma$  is the electric conductivity) [23]. Thus, the values of  $C_0$  ( $C_0 = \mu_r''(\mu_r')^{-2}f^{-1}$ ) should be a constant with varying frequency when the eddy current loss is the main contribution to the magnetic loss [22, 23]. However, the  $C_0$  value increased drastically at first and then decreased with increasing frequency (Fig. 5b). Thus, the magnetic loss of the FeCo/graphene nanocomposite was mainly attributed to the natural ferromagnetic resonance in 2.0–18.0 GHz.

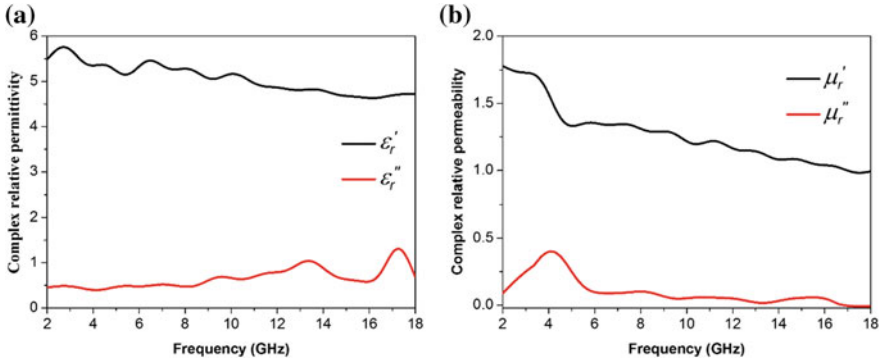


**Fig. 3** Frequency dependences of **a** real and imaginary parts of complex relative permittivity, and **b** real and imaginary parts of complex relative permeability of the FeCo/graphene nanocomposite

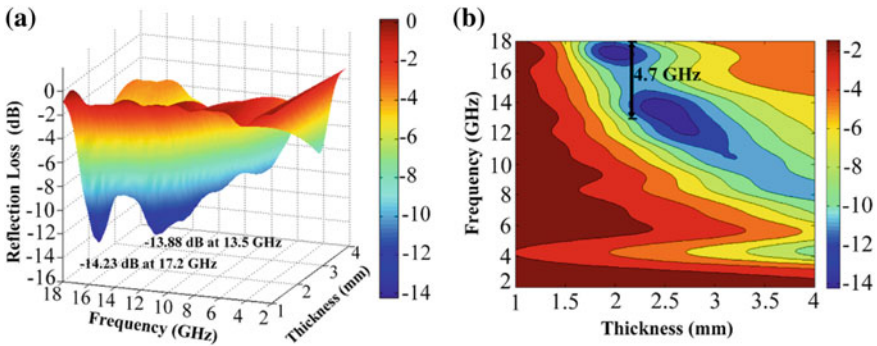


**Fig. 4** **a** Three-dimensional representation and **b** two-dimensional representation of values of reflection loss of the FeCo/graphene nanocomposite

From Fig. 5a, the  $\tan\delta_\epsilon$  values of the FeCo/graphene nanocomposite presented multiple peaks promoting dielectric loss in 5.7–18.0 GHz, but the trough values of  $\tan\delta_\mu$  of the FeCo/graphene nanocomposite exhibited a small inverse resonant behavior accompanying with energy radiation at a similar frequency [24]. The complementary character may lead to an energy transformation between the dielectric loss and magnetic loss in the process of microwave transmission. In general, the dielectric loss is mainly originated from the polarization relaxations of electron, ion and electric dipolar, etc. [25]. The ion and electron polarization usually happens in the very high frequency range of 103–106 GHz [26]. The electric dipolar polarization could be expressed by the following equation [27]:

$$\epsilon_r = \epsilon_\infty + \frac{\epsilon_s - \epsilon_\infty}{1 + j2\pi f\tau} = \epsilon_r' - j\epsilon_r'' \tag{4}$$



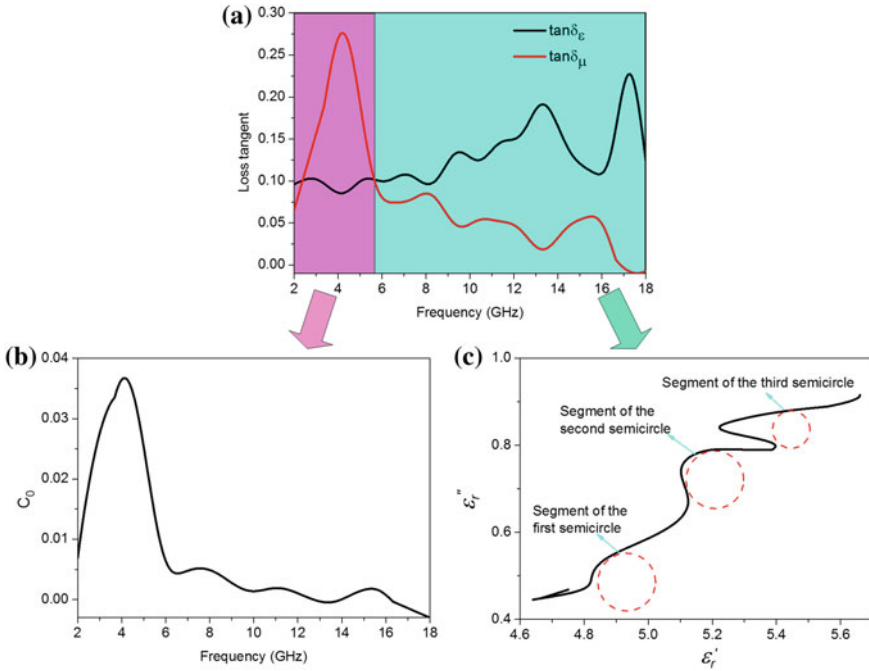


**Fig. 5** **a** Dielectric loss tangent and magnetic loss tangent, **b** plot of  $C_0$  versus frequency, and **c** Cole–Cole curves of the FeCo/graphene nanocomposite

where  $\epsilon_s$ ,  $\epsilon_\infty$  and  $\tau$  are the static permittivity, relative dielectric permittivity at the high-frequency limit, and polarization relaxation time, respectively. Meanwhile,  $\epsilon_r'$  and  $\epsilon_r''$  could be expressed by the following equations:

$$\epsilon_r' = \epsilon_\infty + \frac{\epsilon_s - \epsilon_\infty}{1 + (2\pi f)^2 \tau^2} \tag{5}$$

$$\epsilon_r'' = \frac{2\pi f \tau (\epsilon_s - \epsilon_\infty)}{1 + (2\pi f)^2 \tau^2} \tag{6}$$

According to Eqs. (5) and (6), the relationship between  $\epsilon_r'$  and  $\epsilon_r''$  was deduced as follows:

$$\left( \epsilon_r' - \frac{1}{2}(\epsilon_s + \epsilon_\infty) \right)^2 + (\epsilon_r'')^2 = \frac{1}{4}(\epsilon_s - \epsilon_\infty)^2 \tag{7}$$

Hence, the Cole–Cole semicircle curve can be established by plotting  $\epsilon_r''$  against  $\epsilon_r'$ . As shown in Fig. 5c, the  $\epsilon_r'' - \epsilon_r'$  curve of the FeCo/graphene nanocomposite displayed segments of three semicircles. Each semicircle represented one Debye



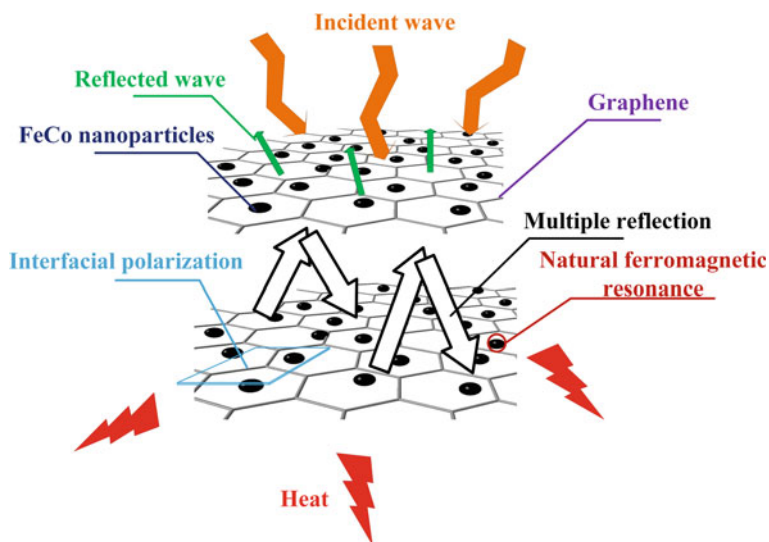


**Fig. 6** Schematic view of microwave absorption mechanisms of the FeCo/graphene nanocomposite

relaxation process, which would effectively enhance the dielectric loss and improve the microwave absorption of the FeCo/graphene nanocomposite.

Figure 6 shows the schematic illustration of the microwave absorption mechanism of the FeCo/graphene nanocomposite. The enhanced microwave absorption properties of the FeCo/graphene nanocomposite can be explained as follows. Firstly, the nanocomposite with uniform dispersion of FeCo nanoparticles and layered graphene sheets promoted multiple reflections, which extended routes of microwave propagation in the nanocomposite and made a contribution to microwave absorption. Secondly, the nanocomposite composed of magnetic FeCo and electrical graphene had improved impedance matching and synergistic effect between permittivity and permeability, which enhanced the absorption ability of the nanocomposite [28]. Thirdly, the multi-interfaces of FeCo and graphene were advantageous to microwave absorption because of the enhanced interfacial polarization. Moreover, the magnetic loss, resulting from the natural ferromagnetic resonance of the FeCo/graphene nanocomposite, would further enhance its microwave absorption. Lastly, the FeCo nanoparticles with the small particle size had perfect chemical activity, promoting the movement of the molecules and electrons, which further dissipated the microwave energy as a result of its transformation to thermal energy [29].

## Conclusions

In summary, microwave-assisted one-step synthesis of the FeCo/graphene nanocomposite was investigated. The FeCo nanoparticles and graphene sheets were obtained simultaneously in the ethylene glycol solvent under microwave irradiation at 190 °C in only 12 min, which was much shorter than the time required by conventional methods. The morphology of the nanocomposite showed that the FeCo nanoparticles with average crystallite size of 40.27 nm were anchored on the surface of graphene sheets. With the filling ratio of only 10 wt% and the thickness of 2.2 mm, the nanocomposite showed the  $RL_{\min}$  of  $-12.56$  dB and the wide  $f_E$  of 4.7 GHz. In addition, the RL values revealed two RL peaks in the frequency range of 2–18 GHz, indicating that the nanocomposite had great microwave absorption property. In particular, the microwave absorption of the nanocomposite was attributed to the synergistic effect of dielectric loss, conductive loss and magnetic loss, in association with its large specific surface area, small size of FeCo nanoparticles, high conductivity of graphene sheets, multiple interfaces, and natural ferromagnetic resonance of FeCo nanoparticles. Due to its high performance, the FeCo/graphene nanocomposite has the potential to serve as a good microwave absorber.

**Acknowledgements** This work was partially supported by the National Natural Science Foundation of China under Grants 51774337, 51504297 and 51811530108; the Natural Science Foundation of Hunan Province, China, under Grant 2017JJ3383; the Key Laboratory for Solid Waste Management and Environment Safety (Tsinghua University) Open Fund under Grant SWMES2017-04; the Project of State Key Laboratory Cultivation Base for Nonmetal Composites and Functional Materials under Grant 17kfk11; the Fundamental Research Funds for the Central Universities of Central South University under Grant 2018zzts799; the Co-Innovation Center for Clean and Efficient Utilization of Strategic Metal Mineral Resources under Grant 2014-405; the Guangdong Guangqing Metal Technology Co. Ltd. under Grant 738010210; the Innovation-Driven Program of Central South University under Grant 2016CXS021; and the Shenghua Lieying Program of Central South University under Grant 502035001.

## References

1. Liu C, Xu Y, Wu L, Jiang Z, Shen B, Wang Z (2015) Fabrication of core-multishell MWCNT/Fe<sub>3</sub>O<sub>4</sub>/PANI/Au hybrid nanotubes with high-performance electromagnetic absorption. *J Mater Chem A* 3:10566–10572
2. Pawar S, Kumar S, Jain S, Gandhi M, Chatterjee K, Bose S (2017) Synergistic interactions between silver decorated graphene and carbon nanotubes yield flexible composites to attenuate electromagnetic radiation. *Nanotechnology* 28:025201–025215
3. Qiang R, Du Y, Zhao H, Wang Y, Tian C, Li Z, Han X, Xu P (2015) Metal organic framework-derived Fe/C nanocubes toward efficient microwave absorption. *J Mater Chem A* 3:13426–13434
4. Wang F, Sun Y, Li D, Zhong B, Wu Z, Zuo S, Yan D, Zhuo R, Feng J, Yan P (2018) Microwave absorption properties of 3D cross-linked Fe/C porous nanofibers prepared by electrospinning. *Carbon* 134:264–273

5. Li Y, Liu R, Pang X, Zhao X, Zhang Y, Qin G, Zhang X (2018) Fe@C nanocapsules with substitutional sulfur heteroatoms in graphitic shells for improving microwave absorption at gigahertz frequencies. *Carbon* 126:372–381
6. Nieto A, Bisht A, Lahiri D, Zhang C, Agarwal A (2016) Graphene reinforced metal and ceramic matrix composites: a review. *Int Mater Rev* 62:241–302
7. Novoselov KS, Fal'ko VI, Colombo L, Gellert PR, Schwab MG, Kim K (2012) A roadmap for graphene. *Nature* 490:192–200
8. Compton OC, Nguyen ST (2010) Graphene oxide, highly reduced graphene oxide, and graphene: versatile building blocks for carbon-based materials. *Small* 6:711–723
9. Lv H, Guo Y, Yang Z, Cheng Y, Wang LP, Zhang B, Zhao Y, Xu ZJ, Ji G (2017) A brief introduction to the fabrication and synthesis of graphene based composites for the realization of electromagnetic absorbing materials. *J Mater Chem C* 5:491–512
10. Gao B, Qiao L, Wang J, Liu Q, Li F, Feng J, Xue D (2008) Microwave absorption properties of the Ni nanowires composite. *J Phys D Appl Phys* 41:235005–235010
11. Yang Y, Xu C, Xia Y, Wang T, Li F (2010) Synthesis and microwave absorption properties of FeCo nanoplates. *J Alloy Compd* 493:549–552
12. Feng Y, Qiu T (2012) Enhancement of electromagnetic and microwave absorbing properties of gas atomized Fe-50 wt%Ni alloy by shape modification. *J Magn Mater* 324:2528–2533
13. Sun G, Wu H, Liao Q, Zhang Y (2018) Enhanced microwave absorption performance of highly dispersed CoNi nanostructures arrayed on graphene. *Nano Res* 11:2689–2704
14. Zhu J, Luo Z, Wu S, Haldolaarachchige N, Young DP, Wei S, Guo Z (2012) Magnetic graphene nanocomposites: electron conduction, giant magnetoresistance and tunable negative permittivity. *J Mater Chem* 22:835–844
15. Guo X, Bai Z, Zhao B, Zhang R, Chen J (2017) Tailoring Microwave-absorption properties of  $\text{Co}_x\text{Ni}_y$  alloy/RGO nanocomposites with tunable atomic ratios. *J Electron Mater* 46:2164–2171
16. Zhang B, Wang J, Tan H, Su X, Huo S, Yang S, Chen W, Wang J (2018) Synthesis of Fe@Ni nanoparticles-modified graphene/epoxy composites with enhanced microwave absorption performance. *J Mater Sci Mater Electron* 29:3348–3357
17. Hummers WS, Offeman RE (1958) Preparation of graphitic oxide. *J Am Chem Soc* 80:1339
18. Che R, Peng L, Duan X, Chen Q, Liang X (2004) Microwave absorption enhancement and complex permittivity and permeability of Fe encapsulated within carbon nanotubes. *Adv Mater* 16:401–405
19. Fu M, Jiao Q, Zhao Y (2013) Preparation of  $\text{NiFe}_2\text{O}_4$  nanorod-graphene composites via an ionic liquid assisted one-step hydrothermal approach and their microwave absorbing properties. *J Mater Chem A* 1:5577–5586
20. Ren L, Huang S, Fan W, Liu T (2011) One-step preparation of hierarchical superparamagnetic iron oxide/graphene composites via hydrothermal method. *Appl Surf Sci* 258:1132–1138
21. Mattevi C, Eda G, Agnoli S, Miller S, Mkhoyan KA, Celik O, Mastrogianni D, Granozzi G, Garfunkel E, Chhowalla M (2009) Evolution of electrical, chemical, and structural properties of transparent and conducting chemically derived graphene thin films. *Adv Funct Mater* 19:2577–2583
22. Peng Z, Hwang JY (2015) Microwave-assisted metallurgy. *Int Mater Rev* 60:30–63
23. Zhang X, Wang G, Cao W, Wei Y, Liang J, Guo L, Cao M (2014) Enhanced microwave absorption property of reduced graphene oxide (RGO)- $\text{MnFe}_2\text{O}_4$  nanocomposites and polyvinylidene fluoride. *ACS Appl Mater Interfaces* 6:7471–7478
24. Zhang X, Guan P, Dong X (2010) Transform between the permeability and permittivity in the close-packed Ni nanoparticles. *Appl Phys Lett* 97:033107–033109
25. Lu M, Cao W, Shi H, Fang X, Yang J, Hou Z, Jin H, Wang W, Yan J, Cao M (2014) Multi-wall carbon nanotubes decorated with ZnO nanocrystals: mild solution-process synthesis and highly efficient microwave absorption properties at elevated temperature. *J Mater Chem A* 2:10540–10547
26. Wen B, Cao M, Hou Z, Song W, Zhang L, Lu M, Jin H, Fang X, Wang W, Yuan J (2013) Temperature dependent microwave attenuation behavior for carbon-nanotube/silica composites. *Carbon* 65:124–139

27. Han M, Yin X, Kong L, Li M, Duan W, Zhang L, Cheng L (2014) Graphene-wrapped ZnO hollow spheres with enhanced electromagnetic wave absorption properties. *J Mater Chem A* 2:16403–16409
28. Chen T, Deng F, Zhu J, Chen C, Sun G, Ma S, Yang X (2012) Hexagonal and cubic Ni nanocrystals grown on graphene: phase-controlled synthesis, characterization and their enhanced microwave absorption properties. *J Mater Chem* 22:15190–15197
29. Reid AHM, Kimel AV, Kirilyuk A, Gregg JF, Rasing Th (2010) Optical excitation of a forbidden magnetic resonance mode in a doped lutetium-iron-garnet film via the inverse Faraday effect. *Phys Rev Lett* 105:107402–107405